Osteogenic differentiation of adipose tissue-derived mesenchymal stem cells on nanostructured Ti6Al4V and Ti13Nb13Zr

Francesca Marini[1]
Ettore Luzi[1]
Sergio Fabbri[1]
Simone Ciuffi[1]
Sabina Sorace[1]
Isabella Tognarini[1]
Gianna Galli[1]
Roberto Zonefrati[1]
Fausto Sbaiz[2]
Maria Luisa Brandi[1]

[1] Department of Surgery and Translational Medicine, University of Florence, Florence, Italy
[2] Lima-Lto spa Medical System, Villanova di San Daniele del Friuli, Udine, Italy

Address for correspondence:
Maria Luisa Brandi, MD, PhD
Full Professor of Endocrinology
Unit of Bone and Mineral Metabolic Diseases
Department of Surgery and Translational Medicine,
University of Florence
Largo Palagi 1
50139 Florence, Italy
Phone: +39-055-7946304 - Fax: +39-055-7946303
E-mail: marialuisa.brandi@unifi.it

Summary

Bone tissue engineering and nanotechnology enable the design of suitable substitutes to restore and maintain the function of human bone tissues in complex fractures and other large skeletal defects. Long-term stability and functionality of prostheses depend on integration between bone cells and biocompatible implants.
Human adipose tissue-derived mesenchymal stem cells (hAMSCs) have been shown to possess the same ability to differentiate into osteoblasts and to produce bone matrix of classical bone marrow derived stem cells (BMMSCs).
Ti6A14V and Ti13Nb13Zr are two different biocompatible titanium alloys suitable for medical bone transplantation. Preliminary results from our Research Group demonstrated that smooth Ti6Al4V surfaces exhibit an osteoconductive action on hAMSCs, granting their differentiation into functional osteoblasts and sustaining bone matrix synthesis and calcification.
The purpose of this study is to assay the ability of nanostructured Ti6Al4V and Ti13Nb13Zr alloys to preserve the growth and adhesion of hAMSCs and, mostly, to sustain and maintain their osteogenic differentiation and osteoblast activity.
The overall results showed that both nanostructured titanium alloys are capable of sustaining cell adhesion and proliferation, to promote their differentiation into osteoblast lineage, and to support the activity of mature osteoblasts in terms of calcium deposition and bone extracellular matrix protein production.

KEY WORDS: nanostructured titanium alloys; mesenchymal stem cells; adipose tissue; osteogenic differentiation; bone regeneration.

Introduction

Long-term stability of orthopedic bioimplants, as well as bone tissue function restoration, depends principally on the integration between the implant and the native bone tissue. Establishing and maintaining normal bone regeneration at the bone-device interface is the critical issue for the long-term success of bone implants. Several variables influence biocompatibility, proliferation, and osteogenic differentiation on hard biomaterials, such as chemical composition, surface shape and nanoscale features (1). The cytocompatibility of a biomaterial is strongly connected to chemical composition, while the biomaterial three-dimensional structure (topography, geometry, roughness, and particle size) plays a crucial role in guaranteeing its interaction with host cells (2). In particular, the surface topography (size, shape, and surface texture) of a biomaterial is one of the most important parameters that influence cellular attachment, adherence, proliferation and migration, and also differentiation and survival of different cell types (3-9). The creation of biomaterial surface nanoscale characteristics surely improves the initial interlocking of the implant and bone tissue. Recently, the progressive application of nanostructured surfaces in medicine has become a common approach to increase the cytocompatibility and osteointegration of orthopaedic and dental implants (10).
Titanium (Ti) alloys are well known for their superior mechanical properties as well as for their good biocompatibility, making them desirable as surgical implant materials. The reason for the extended use of Ti and its alloys as implant biomaterials stems from their lower elastic modulus, superior biocompatibility, and improved corrosion resistance compared to the more conventional stainless steel (11).
Recently, the effects of surface properties of microstructured and nanostructured titanium-based biomaterials have been *in vitro* analysed regarding their inductive and conductive osteogenic potential. Human mesenchymal stem cells (MSCs) have shown to be able to differentiate into osteoblasts if cultured on Ti surfaces with microscale roughness even in absence of osteogenic components within the culture medium (12). Some *in vitro* studies, investigating the response of adherent cells to nanography surfaces, indicated that different cell phenotypes have different levels of sensitivities (13-16). In addition, an enhanced collagen production has been demonstrated, as well as increased ALP activity and calcium deposition of osteoblasts cultured on nanoparticulate Ti6Al4V (17, 18). To date, however, no data are available on the influence of a nanostructured hard biomater-

ial on osteogenic differentiation of not classical tissue-derived MSCs.
The aim of this study was to examine the ability of two different nanostructured Ti alloys (Ti6Al4V and Ti13Nb13Zr) to support growth, adhesion, osteogenic differentiation and osteoblast activity of adipose tissue-derived mesenchymal stem cells (AMSCs). A previous study by our Research Group has demonstrated that AMSCs possess the same ability to differentiate into osteoblastic lineage and to produce bone matrix of the bone marrow-derived stem cells (BMMSCs) and that smooth Ti6Al4V surfaces exhibit an osteoconductive action on AMSCs, granting their differentiation into functional osteoblasts and sustaining bone matrix synthesis and calcification (19).
The present study assayed the ability of nanostructured Ti6Al4V and Ti13Nb13Zr to substain and maintain growth and osteogenic differentiation of three primary cultures of AMSCs, using polystyrene (PS) and normal human osteoblast primary cells (NHOst), respectively, as culture substrate and cell controls.

Materials and methods

The materials used in this study were purchased from Sigma-Aldrich (St Louis, MO, USA), unless otherwise specified.

Preparation and surface characterization of nanostructured Ti alloy samples

Nanostructured Ti6Al4V and Ti13Nb13Zr alloys (Lima-Lto spa Medical Systems, San Daniele del Friuli, Udine, Italy) were obtained by a production process called Mechanomaking, followed by a hot extrusion of the obtained powders. The Mechanomaking process is a high energy milling technology for powder materials. This flexible process allows the manufacturing of nanophase materials (crystal size <100nm) with a combination of mechanical actions on the particles (mechanical mixing, elasto-plastic deformation, microwelding, fractures, etc.) and chemical actions (diffusion, bond breaks, chemical activation, generation of activated state and free radicals, etc.). This process uses chemical mechanical reactors in which the introduced materials in powder form are subjected to high-frequency chemical mechanical actions by means of milling. The process usually takes place at room temperature (RT).
Ti alloy specimens (squared plates of 15 x 15 mm with 1.5 mm thickness) were prepared by bar electro-cutting, mechanically polished with silica paper and diamond grinding paste, etched with Kroll's solution (6% of nitric acid and 2% of hydrofluoric acid in distilled water), cleaned in ultrasound bath and rinsed in deionised water. The surface of the specimen was then characterized for roughness and structural composition using Taylor-Hobson Talisurf and Quanta 200 Environmental Scanning Electron Microscope (ESEM, FEI-Italy) respectively. Surface characterizations of nanostructured Ti6Al4V and Ti13Nb13Zr were performed evaluating the three roughness parameters: Ra (arithmetic mean value), Rt (mean-square-average) and Rq (maximum roughness height). A total of 15 measurements on different components were performed to obtain roughness averages and standard errors. Structural composition was evaluated using back-scattered electron detector (BSE), while qualitative analysis and relative mapping of element distribution were studied by energy dispersion spectroscopy (EDS).

Cell cultures

Subcutaneous adipose tissue biopsies were collected from subjects, undergoing surgery, before the establishment of the Ethics Committee at the "Azienda Ospedaliera Universitaria Careggi''. All derived cell lines were handled in a totally anonymous way.
Primary cultures of AMSCs (PA1, PA2, and PA3 cell lines) were isolated as follows: each adipose tissue sample was minced into small pieces (about 1 mm) and digested for 3 hours (h) at 37°C in Ham's F12 Coon's modification medium supplemented with 20% fetal bovine serum (FBS) and 3 mg/ml collagenase type I (C-0130). Afterwards, the tissue was mechanically dispersed and passed through a 230-μm stainless steel tissue sieve, and the fraction containing the pre-adipocytes was incubated with an erythrocyte lysis buffer for 2 min at RT. The cells were cultured in 100 mm culture plates at 37°C in humid atmosphere with 5% CO_2 in growth medium (GM: Ham's F12 Coon's modification medium supplemented with 10% FBS, 100 IU/ml penicillin, 100 µg/ml streptomycin and 1 ng/ml basic Fibroblast Growth Factor). The medium was refreshed twice a week, and cells were used for further subculturing or cryopreservation upon reaching 5 x 10^3 cells/cm^2. Cells used in subsequent experiments were between the 3rd and the 7th passage. Characterization of AMSC cell lines to verify their multi-potency was performed by monitoring the expression/lack of expression of specific markers (CD34, CD44, CD45, CD71) through flow cytometry, and by studying the adipogenic and osteogenic induction as previously described (18).
The normal human osteoblast primary cells (NHOst) was purchased from Lonza (Lonza Walkersville, MD, USA) and used as control cell line. Cells were cultured in GM incubated at 37°C in humidified atmosphere with 5% CO_2 until confluence, then detached with trypsin/EDTA acid solution and plated at the desired density in the appropriate medium for each experiment.

[^{3}H]-thymidine incorporation assay

Cell growth and viability on PS and nanostructured Ti alloys were assessed by [^{3}H]-thymidine incorporation assay both on NHOst and AMSCs. Cells were seeded at semi-confluence on polystyrene (PS) or nanostructured Ti alloys in GM. After 24 h the medium was substituted with a fresh one supplemented with 0.1% FBS. After 72 h the cells were incubated with GM for 24 h, then with [^{3}H]-thymidine (2 µCi/ml in GM final concentration) for 4 h. The medium was removed, and the cells were washed three times with Dulbecco's Phosphate Buffered Saline (DPBS, BioWhittaker), and then fixed in 5% trichloroacetic acid (TCA) for 10 minutes (min) at 4°C. The supernatant was discarded, the plates were air-dried and the cells were lysed with 0.5 N NaOH (500 µl/well) at 80°C for 60 min. The lysate was added with Hionic-Fluor liquid scintillation cocktail (PerkinElmer, Waltham, MA, USA) and the radioactivity was counted in a β-counter (Packard Instrument Company, Meridien, CT, USA) and expressed as disintegrations per minute (DPM)/cm^2.

Osteogenic differentiation

Cells were plated on PS, Ti6Al4V, or Ti13Nb13Zr at a cell density of 1 x 10^4 cells/cm^2 in GM and grown to 70-80% confluence. Afterwards, the medium was switched to the following osteogenic medium (OM): Ham's F12 Coon's modification medium supplemented with 10% FBS (South America origin, BioWhittaker), 100 IU/ml penicillin, 100 µg/ml strepto-

mycin, 10 nM dexamethasone, 0.2 mM sodium L-ascorbyl-2-phosphate, and 10 mM β-glycerol phosphate. The medium was refreshed twice a week.
The alkaline phosphatase (ALP) activity was determined in AMSCs and NHOst cells cultured on nanostructured Ti alloys or on PS at 1, 10, 20, and 40 days after osteogenic induction by both fluorometric assay and cytochemical staining, as previously described (19).

Immunocytochemistry of bone matrix proteins
AMSCs and NHOst cells were maintained for 1, 4, 20, and 40 days on nanostructured Ti alloys in OM, using PS as control. Experiments have been repeated in quadruplicate, using four different samples for each material (Ti6Al4V, Ti13Nb13Zr, and PS).
Cells were fixed in 4% paraformaldehyde (PFA)/DPBS for 20 min and permeabilized in 0.5% Triton X-100/DPBS for 10 min at room temperature *(RT*). Non-specific binding sites were blocked with 2% bovine serum albumin (BSA)/DPBS for 30 min at *RT*.
Extracellular bone matrix protein synthesis has been evaluated by immocytochemistry as follows: cells cultured for 1 and 40 days in OM were antibody-stained for osteocalcin (OCN), for α type I collagen (COLIA1) and for osteopontin (OPN); for OCN staining, however, before permeabilization, cells were decalcified with 9% EDTA in Tris-HCl 50 mM pH 7.5 for 5 min. The primary antibodies used were anti-COLIA1 (1:80 in 2% BSA, polyclonal anti-human raised in rabbit, Abcam, Cambrige, UK, 60 min), OC4-30 (1:10 in 2% BSA, monoclonal anti-human raised in mouse, Genetex, San Antonio, TX, USA, overnight), and anti-OPN (1:100 in 2% BSA, polyclonal anti-human raised in goat, 60 min). The secondary antibodies used were FITC anti-rabbit IG antibody (1:100 in 2% BSA) for COLIA1, FITC anti-mouse IG antibody (1:100 in 2% BSA, Chemicon) for OCN, and Alexa Fluor 555 anti-goat IG (1:200 in 2% BSA, Molecular Probes, Eugene, OR, USA) for OPN.

Extracellular matrix mineralization
Mineralization of the extracellular matrix by AMSCs and NHOst cultured on nanostructured Ti alloys or on PS was evaluated at 1, 20, 40, and 60 days after osteogenic induction by both calcein staining and Alizarin Red S assay, as previously described (18).

Cell morphology analysis
Cell morphology and cytoskeleton organization on PS and nanostructured Ti6A14V and Ti13Nb13Zr alloys have been evaluated by β-actin labelling with TRITC-Phalloidin and analysis of β-actin filament number and cellular distribution. Samples were incubated with 10 μg/ml of TRITC-Phalloidin in 2% BSA/DPBS for 30 min, rinsed three times with DPBS, and mounted in polyvinyl alcohol mounting medium with antifading DABCO (Fluka Chemie). Images were captured using LSM510 Meta Confocal Microscope, LSCM (Carl Zeiss, Oberkochen, Germany).

Cell adhesion analysis
Cell adhesion on PS and nanostructured Ti6A14V and Ti13Nb13Zr alloys has been evaluated by immunocytochemisty for vinculin adhesion protein as follows: samples cultured for 4 days in OM were stained for vinculin using anti-vinculin primary antibody (1:100, monoclonal anti-human raised in mouse, clone 7F9, Chemicon, Temecula, CA, USA) in 2% BSA/DPBS for 40 min at *RT*. Revelation was obtained using FITC anti-mouse IG antibody (1:100 in 2% BSA/DPBS, Chemicon) for 60 min at *RT*. Cell nuclei were counterstained with TOTO-3 iodide (5 μM, Molecular Probes) for 30 min at RT, after RNAse digestion (200 μg/ml in DPBS), or Hoechst 33258 (1μg/ml in DPBS) for 5 min at *RT*. Samples were rinsed with DPBS (3X) between each step, and mounted in polyvinyl alcohol mounting medium with antifading DABCO (Fluka Chemie). Images were captured using LSM510 Meta Confocal Microscope, LSCM (Carl Zeiss, Jena, Germany).
The ratio of focal contact area (*FCA*) to total cellular area (*TCA*) was calculated for every cell line, grown on Ti6Al4V, Ti13Nb13Zr or PS. *FCA* and *TCA* were respectively evaluated by measuring the average area of focal contacts and the average spread area per cell. The image analysis to obtain *FCA* and *TCA* values was performed following the method described by Hunter et al. (20). Images of cells, immunostained as previously described, were acquired with LSCM and analyzed using CellProfiler image analysis software (www.cellprofiler.org) (21). The data were expressed as means ± SD of a minimum of 100 randomly selected cells for each sample. The degree of cell adhesion was evaluated by calculating the *FCA/TCA* ratio.

Statistical analysis
All the experiments have been performed with the three AMSCs cell lines, and representative average results are reported. For [^{3}H]-thymidine incorporation assay, ALP fluorometric assay, and Alizarin Red S assay, the experiments were carried out in triplicate, and data expressed as means ± SD of quadruplicate experimental points. Statistical differences among mean values were analyzed using Scheffe's test (Statistica 5.1; Statsoft Inc, Tulsa, OK, USA). The statistical significance of differences in the cell adhesion between PS and nanostructured titanium alloys was evaluated by Student's t-test in Excel software (version for PC; Microsoft Corporation, Redmond, WA, USA) on experiments carried out in quadruplicate. Significance has been considered with $p<0.01$.

Results

Surface characterization of nanostructured titanium alloy samples
The values of the roughness parameters showed a significant difference in the average value of surface roughness between the two Ti alloys. In detail, Ti6Al4V samples exhibiting lower Ra and Rt values resulted smoother than Ti13Nb13Zr specimens (Table 1).
BSE micrograph of nanostructured Ti6Al4V surface shows the presence of little clear spots (Figure 1, panel A) that were assigned to Vanadium (Figure 1, panels C and E) by relative mapping distribution with EDS analysis (Figure 1, panel G). BSE micrograph of nanostructured Ti13Nb13Zr surface shows the presence of electrondense spots (Figure 1, panel B) that were assigned to Zirconium (Figure 1, panel D) and Niobium (Figure 1, panel F) by relative mapping distribution with EDS analysis (Figure 1, panel H).
EDS qualitative analysis shows the nanostructured Ti6Al4V spectra (Figure 1, panel G), with emission of Al peak at 1.485 KeV, Ti peak at 4.509 KeV, and V peak at 4.950 KeV, and the Ti13Nb13Zr spectra (Figure 1, panel H), with emission of Zr peak at 2.040 KeV, Nb peak at 2.164 KeV, and Ti

Table 1 - Roughness parameters of the nanostructured Ti alloy samples.

	Ti6Al4V			Ti13Nb13Zr		
Roughness parameters	Ra	Rq	Rt	Ra	Rq	Rt
Average of 15 different measurements	0.0587	0.0826	0.4347	0.2754	0.3341	1.6534
Standard error	0.0032	0.0045	0.0210	0.0379	0.0399	0.1543

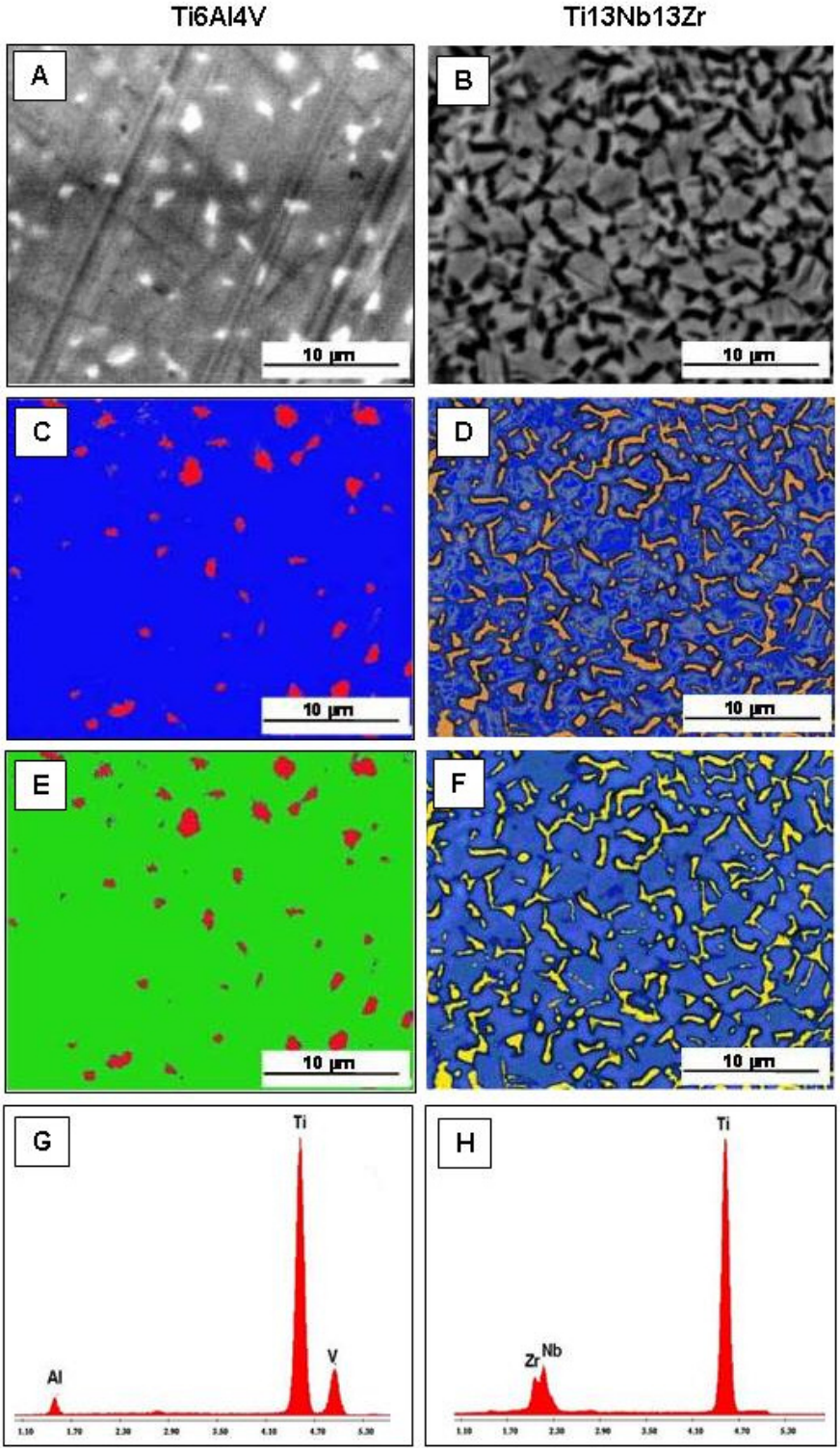

Figure 1 - **Evaluation of structural composition of Ti alloys.** Back-scattered electron detector (BSE) micrograph and relative elemental mapping distribution (panels A-F), and energy dispersion spectroscopy (EDS) qualitative analysis (panels G,H). Notes: Blue = Ti, Green = Al, Red = V, Yellow = Nb, and Orange = Zr.

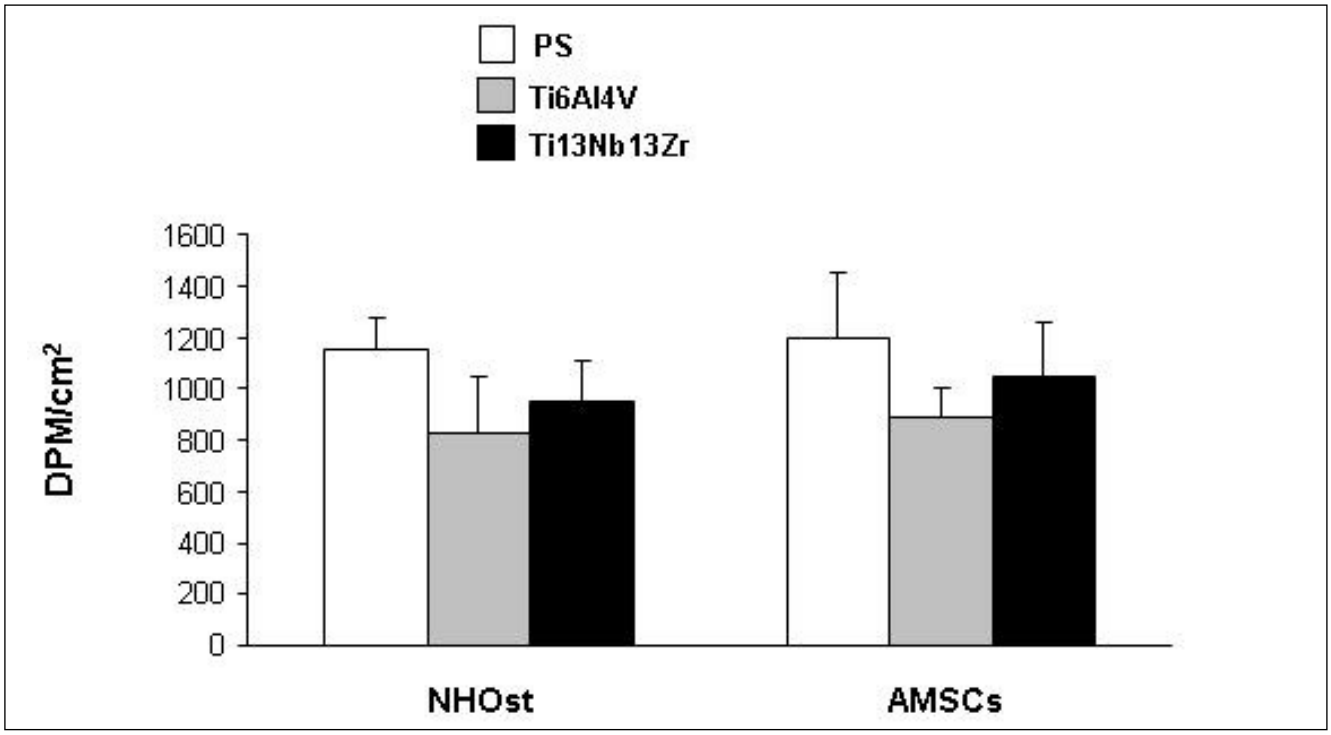

Figure 2 - Analysis of cell growth and viability by [3H]-thymidine incorporation assay in NHOst cells and AMSCs cultured on PS and nanostructured Ti alloys.

peak at 4.509 KeV confirming the elemental composition of each titanium alloy.

Cell growth and viability

All cell lines showed good viability and growth activity on both of the nanostructured Ti alloys (Figure 2).

Cell morphology and adhesion

On all the three tested surfaces, NHOst cells appeared flattened and spread with an oval morphology and small cellular extensions (Figure 3, panels A-C), while AMSCs were spindle or polygonal-shaped with the emission of long cellular extensions (Figure 3, panels D-F). On PS, both NOHst and AMSC cell lines showed a cytoskeleton organization characterized by β-actin bundles running parallel or slightly oblique to the major axis of the cell body (Figure 3, panels A and D). All cells grown on nanostructured Ti6A4IV showed a β-actin cytoskeleton organization similar to that observed on PS (Figure 3, panels B and E). In NHOst and AMSC cells cultured on nanostructured Ti13Nb13Zr, the β-actin cytoskeleton acquired a quite different organization. The cells presented an increased number of β-actin bundles with a segmented and shorter structure, often localized along the lateral borders of the cells (Figure 3, panels C and F).

Regardless of the surfaces, NHOst differed from AMSCs for the distribution and morphology of the focal adhesions. On all the substrates, NHOst cells were characterized by dot-shaped adhesions dispersed throughout the cell body and dash-shaped adhesion at the cell edges (Figure 3, panels G-I), while AMSCs showed larger wire-shaped adhesions, mostly localized at cellular extensions and at cell-to-cell contacts (Figure 3, panels J-L). The intensity of stain increased in all cells growing on Ti13Nb13Zr (Figure 3, panels I and L).

NHOst and AMSC cells each had a different ability to spread and form focal contacts on the different substrates. As a matter of fact, no significant differences were observed for *TCA* values in NHOst cells cultured on each support, whereas AMSCs grown on PS showed statistically significant higher *TCA* levels than cells grown on nanostructured biomaterials. Furthermore, AMSCs on Ti6Al4V were found to have a significantly lower mean *TCA* than cells on Ti13Nb13Zr. With regard to the ability to form focal contact, NHOst cells on nanostructured Ti alloys had a significantly larger area of vinculin localization per cell than cells on PS. In addition, NHOst grown on Ti13Nb13Zr had a significantly higher mean *FCA* than cells on Ti4Al6V. In AMSCs there was no difference for *FCA* value between cells grown on PS and Ti6Al4V, while cells on Ti13Nb13Zr showed a significantly higher mean value of *FCA* than cells grown on the other tested materials. Despite the different behaviours observed between NHOst and AMSC cells, all cells cultured on nanostructured Ti surfaces showed significantly higher *FCA/TCA* ratios, and therefore a higher degree of adhesion than cells grown on PS (Figure 4). The highest *FCA/TCA* values were observed when cells were grown on Ti13Nb13Zr.

Osteogenic differentiation

The cytochemical staining of ALP activity showed that non-induced AMSCs were less committed to the osteoblastic phenotype compared to NHOst cells (percentage of osteoblast committed cells at 1 day from osteogenic induction of 6 ± 2% in AMSCs without significant differences among the three cell lines, and 61 ± 5% in NHOst (data not shown). The lesser commitment of AMSCs was confirmed by the evaluation of ALP activity with 5.0 ± 1.4 μU/μg DNA for AMSCs compared to 45.8 ± 4.8 μU/μg for NHOst at 1 day of osteogenic induction. Both AMSCs and NHOst showed a statistically significant greater mean increase of ALP activity during induction, on PS, compared to that observed on both nanostructured Ti alloys (Figure 5). No differences in the

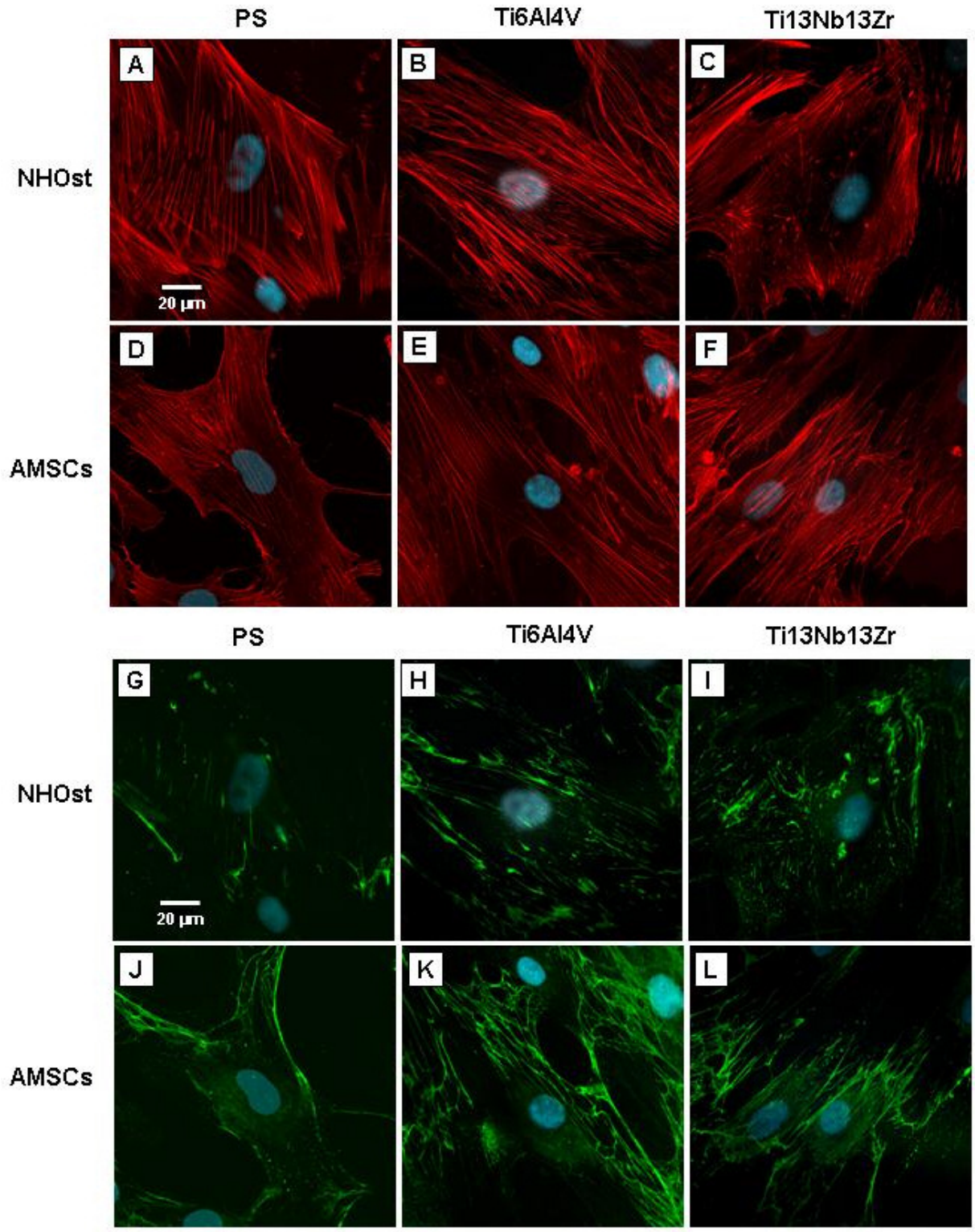

Figure 3 - **Cell morphology, cytoskeleton organization and focal cell adhesion, analysed by β-actin and vinculin immunostaining.** Representative fluorescence images of cytoskeleton β-actin (panels A-F) and focal adhesion protein vinculin (panels G-L) in NHOst cells and AMSCs cultured on PS or nanostructured Ti alloys, after 4 days from osteogenic induction. Notes: Red = actin, green = vinculin, and blue = nuclei.

ALP activity were observed in NHOst and AMSCs grown on Ti6Al4V or Ti13Nb13Zr. However, for NHOst cells the ALP activity slightly increased until the 20th day of induction, on all the three tested surfaces, and then decreased thereafter, while for AMSCs the ALP activity constantly increased up to 40 days from osteogenic induction.

A

	NHOst			AMSCs		
	PS	Ti6Al4V	Ti13Nb13Zr	PS	Ti6Al4V	Ti13Nb13Zr
$\overline{TCA}$(µm)	3415±615	2917±581	2885±957	2077±305	1330±393 *	1662±137 * #
$\overline{FCA}$(µm)	265±94	461±104 *	717±210 * #	386±77	383±92	675±339 * #
$\overline{FCA/TCA}$	0.078±0.026	0.161±0.036	0.261±0.069	0.197±0.041	0.284±0.082	0.429±0.120

B

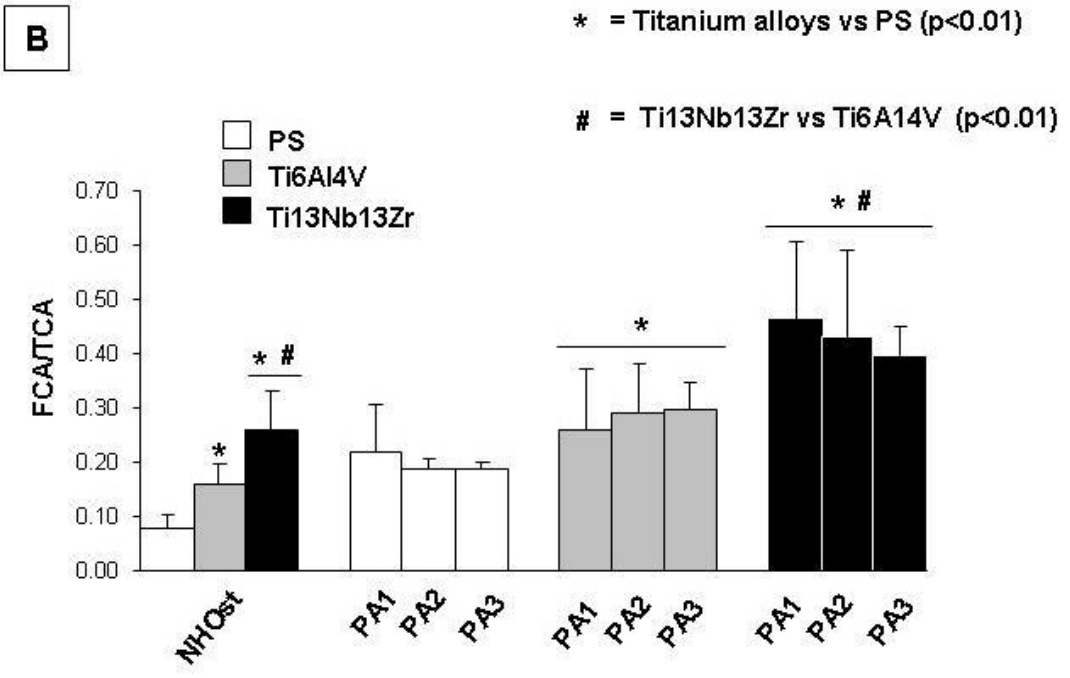

Figure 4 - **Analysis of focal adhesion contacts of cells cultured on PS or nanostructured Ti6Al4V and Ti13Nb13Zr after 4 days from osteogenic induction.** Panel A shows the mean ± standard deviation (SD), in four replicates, of TCA, FCA, and FCA/TCA ratio per cell of NHOst and AMSCs. Panel B shows the graphic representation of FCA/TCA ratio in NHOst and AMSCs on PS or nanostructured Ti alloys. Notes: * = nanostructured titanium alloys vs PS (p<0.01); # = Ti13Nb13Zr vs Ti6Al4V (p<0.01).

Extracellular matrix mineralization

Calcein staining of the produced mineralized matrix evidenced an abundant deposition of hydroxyapatite (HA) crystals 40 days after osteogenic induction on both PS and nanostructured TI alloys (Figure 6). Interestingly, the staining revealed that AMSCs showed a different mineralization pattern on the differ-

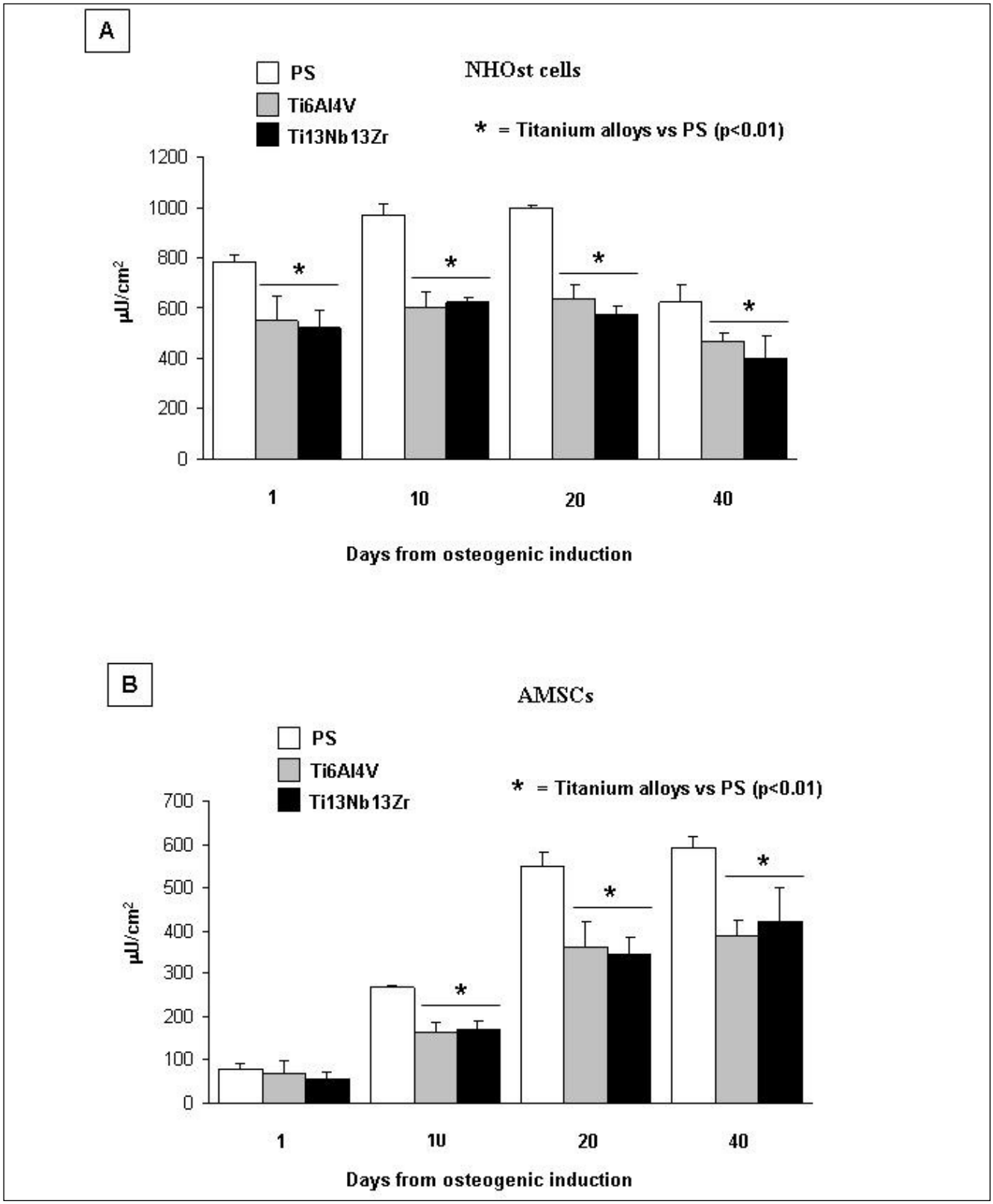

Figure 5 - **Effect of nanostructured Ti6Al4V and Ti13Nb13Zr alloys on ALP activity.** Fluorometric assay for alkaline phosphatase (ALP) activity in NHOst (panel A) and AMSCs (panel B) cells cultured on PS or Ti alloys.
Note: * = nanostructured titanium alloys *vs* PS (p<0.01).

ent surfaces. Forty days after induction, PA cells cultured on PS formed nodules of different sizes spread over large areas throughout the cell monolayer, whereas PA cells grown on Ti nanostructured alloys produced huge ribbon-shaped and interconnected calcified crystals (Figure 6, right panels). This mineralization pattern was similar to that observed in NHOst cells

which deposited smaller mineralized nodules with a needle-like morphology on any examined surface (Figure 6, left panels).

The measurement of calcium content obtained by Alizarin Red S assay showed that, during induction, NHOst cells deposited

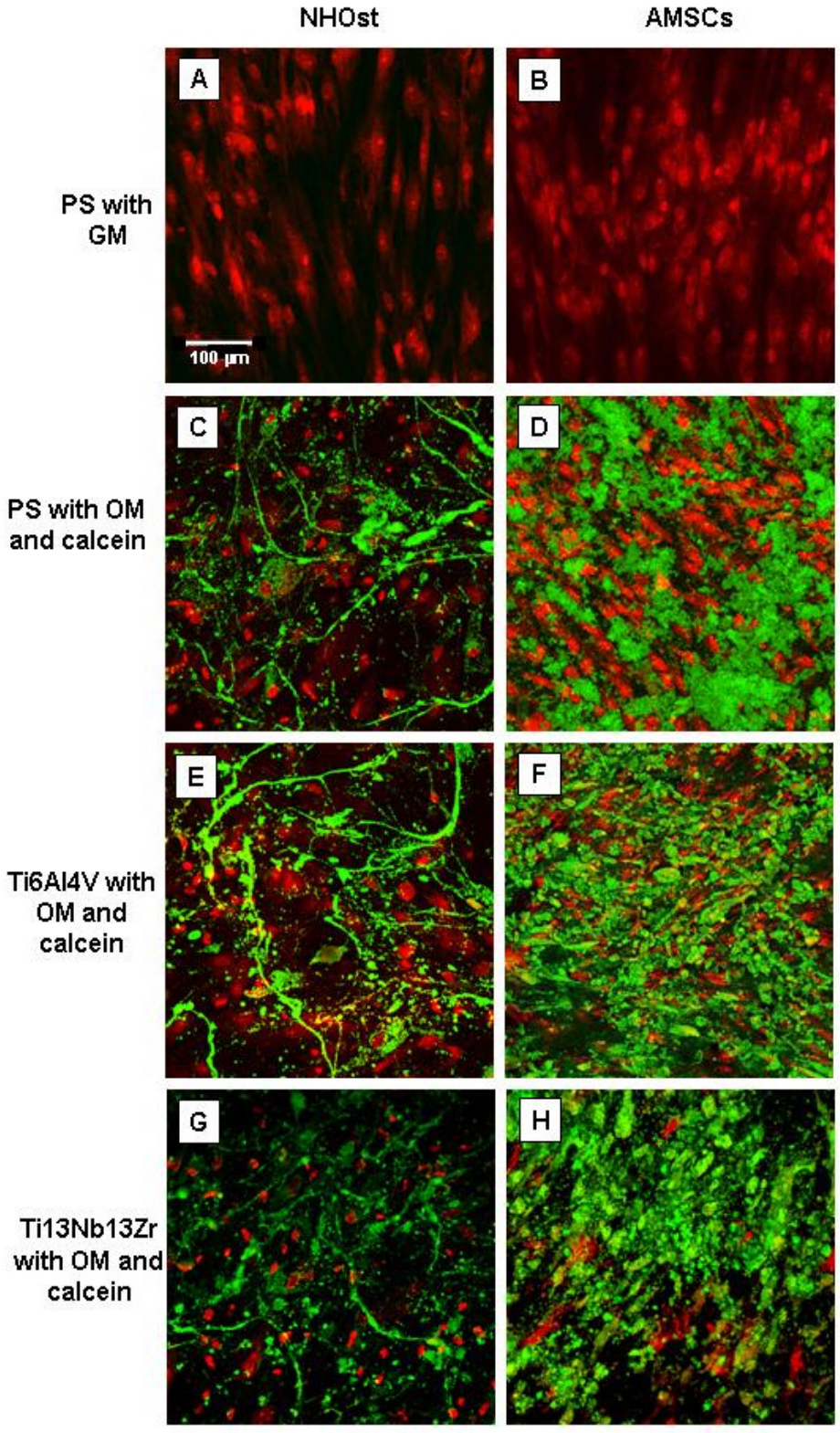

Figure 6 - **Osteoblast activity evaluation by calcein-based measurement of mineral matrix deposition.** Representative fluorescence images of calcium deposits of NHOst (left panels) and AMSCs (right panels) cells cultured on PS (panels A-D) or nanostructured Ti alloy (panels E-H). Panels A and B show, respectively, non-induced NHOst and AMSCs cultured in growth medium (GM). Panels C-H show cell lines cultured on the three different substrates with osteogenic medium (OM) added with 1 µg/ml calcein; cells have been analysed after 40 days from osteogenic induction. The images were a projection of 20-40 images in a stack with 2 µm z-steps. The different number of images in z-stack was determined according to the vertical height of the mineralized deposits. Note: red = nuclei, green = calcium deposits.

a significantly higher amount of calcium mineral content (expressed as µg HAµg DNA) on PS than Ti alloys at 40 and 60 days after induction. The maximal calcium deposition was detected at 40 days after induction on PS. Moreover, no differences between nanostructured Ti6Al4V and Ti13Nb13Zr were observed (Figure 7, panel A). On the contrary, AMSCs produced a constant increasing amount of HA throughout all the induction period on all growth supports. Furthermore, these cell lines, at 40 days after induction, showed significantly higher values of calcium content on nanostructured alloys than PS, without differences between Ti6Al4V and Ti13Nb133Zr (Figure 7, panel B). Sixty days after induction, no differences in the cal-

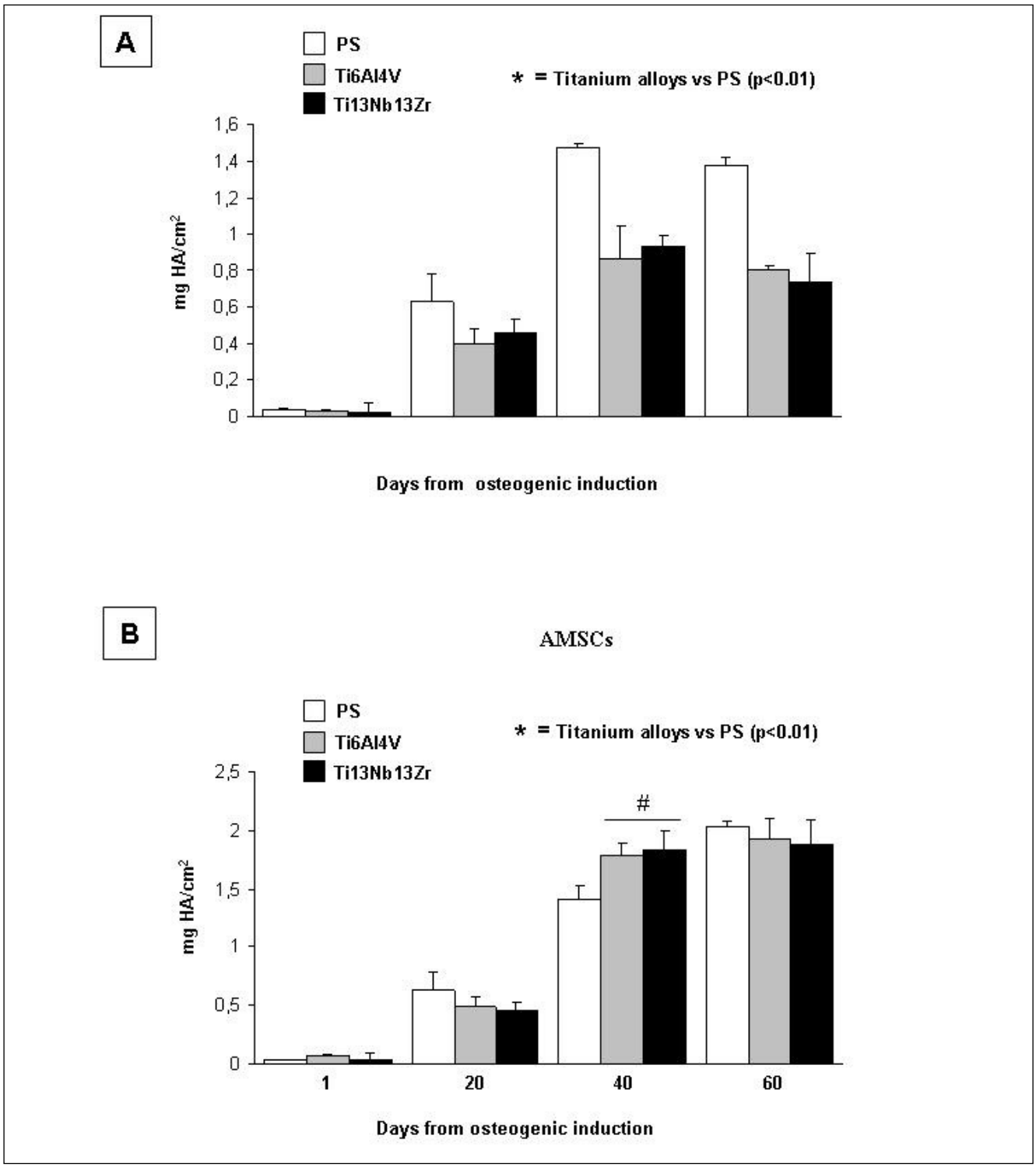

Figure 7 - **Osteoblast activity evaluation by measurement of mineral calcium deposit contents by Alizarin Red S assay.** Alizarin Red S assay in NHOst (panel A) and AMSCs (panel B) cultured on PS or Ti alloys.
Note: * = nanostructured titanium alloys *vs* PS (p<0.01).

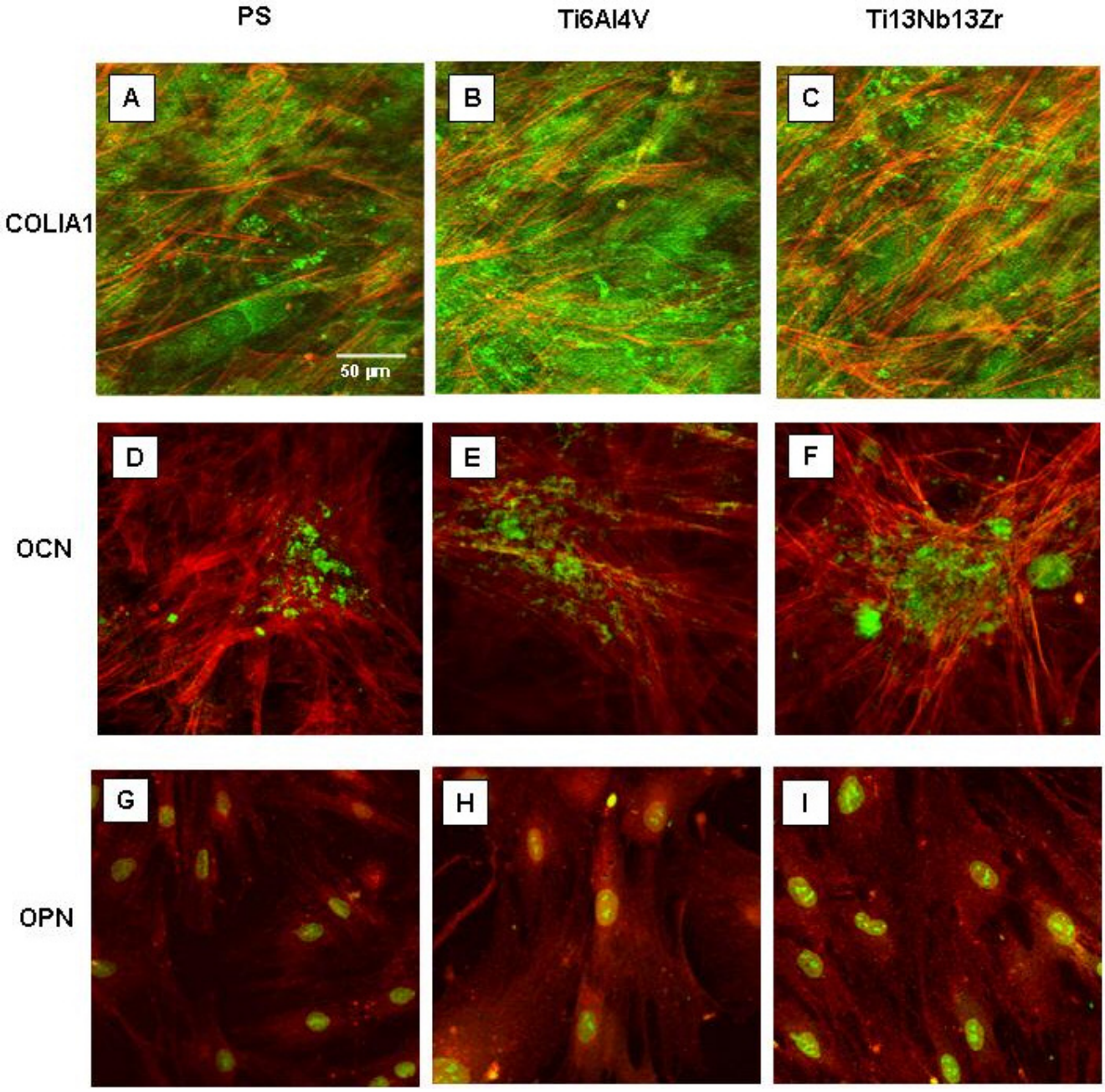

Figure 8 - **Osteoblast activity evaluation by immunostaining of COLIA1, OCN and OPN proteins.** COLIA1, OCN, and OPN representative fluorescence images for AMSCs after 40 days from osteogenic induction cultured on PS or nanostructured Ti alloys.
Notes: red = actin (panels A-F) or OPN (panels G-I), and green = COLIA1 (panels A-C), OCN (panels D-F) or nuclei (panels G-I).

cium deposition were observed in AMSCs grown on the three growth supports.

Analysis of extracellular matrix proteins

Osteoblastic activity was confirmed by OPN, OCN, and COLIA1 immunostaining (Figure 8). A faint cytoplasmic staining for OPN and COLIA1 was detected in all non-induced cells, while no signal for OCN was observed before induction (data not shown). Osteogenic induction promoted an increase of OPN and COLIA1 production and *the synthesis ex novo* of OCN in all cells. In detail, after 40 days of culture in OM, both NHOst and AMSCs were observed to form a COLIA1 network in the extracellular matrix and dense OCN and OPN positive aggregates reminiscent of bone nodule structures. After induction, no significant difference was observed in COLIA1 and OCN staining in each cell line cultured on different substrates, while OPN staining appears more intense both in NHOst and AMSCs cultured on both the Ti alloys than on PS.

Discussion

Repairing gross bone defects and restoring and maintaining

the normal function of bone tissue are the great challenges of orthopedic and oral-maxillofacial surgery. Until few years ago, the gold standard for the reconstruction of large bone tissue defects has been the autologous bone graft from the patient or the allogenic bone graft from a donor. However, these techniques present complications (i.e. morbidity and chronic pain at the donor site, infection, hypersensitivity, reduced integration with the native tissue, increased bone resorption at the implant site, etc.) in about 10-30% of patients (22), and for decades there has been a search for more suitable alternatives.

Bone tissue engineering is an emerging discipline that applies the principles of biology and engineering to the development of viable substitutes for long-term bone tissue replacement and restoration of the best possible tissue and organ functionality. This approach includes the use of synthetic biocompatible scaffolds that can be integrated to the host native bone tissue, allowing the substitution of lost bone and the restoration of bone tissue function. Long-term stability of bone implants depends on integration between the chosen biomaterial and the host bone cells, particularly osteoblasts.

Ti implants are widely used as bone substitutes in dental and orthopaedic surgery thanks to their excellent mechanical properties, corrosion resistance, low density, and good biocompatibility. Ti6Al4V currently represents a widely used material mainly in total joint replacement implants thanks to its excellent mechanical and anti-corrosive properties, but it contains vanadium which is known to be cytotoxic (23). Consequently, alloys of new composition, such as Ti13Nb13Zr, have recently been developed for biomedical applications.

Anyway, smooth Ti surfaces present low cytocompatibility and reduced cell integration properties. Osteointegration can be implemented by Ti microfeature modifications, such as the increase of roughness, by generation of nanostructured surfaces and by surface mineralization with calcium apatite (24), which favour bone cell adhesion, and can maintain bone growth and normal remodelling in the area of the implant.

A study investigated the effect of nanocristalline hydroxyapatite coating of Ti13Nb13Zr on the morphology, proliferation and osteogenic differentiation of human BMMSCs, evidencing that the presence of coating induces MSC osteogenic differentiation with increased production of collagen type I, osteopontin and osteonectin (25). No study is available on the role of nanostructured Ti13Nb13Zr on osteoblast differentiation and activity.

One recent work has investigated the effects of nanoscale features and roughness of Ti6Al4V on osteoblast differentiation, finding that nanostructured Ti6Al4V osteogenic properties are strongly related to the different stage of preosteoblast cell differentiation (26).

However, the long-term integration between the implant and the host bone tissue does not only include the physical and chemical modification of the implant surface or its adsorption with osteogenic bioactive molecules, but also the use of cell-based therapies involving MSCs, able to continuously differentiate into osteoblasts. Bone marrow has been widely considered the most abundant source of MSCs, but recently also MSCs derived from adipose tissue have gained growing attention thanks to their ability to differentiate into osteoblasts, and their easy accessibility in great amounts via simple and non-invasive subcutaneous biopsy. A previous study by our Research Group demonstrated that human AMSCs, like their mesenchymal counterpart in bone marrow, have an extensive proliferative potential, can differentiate toward osteogenic lineage and are able to produce bone matrix (19), and that smooth Ti6Al4V surfaces exhibited an osteoinductive action on these cells. Nevertheless, no studies are available on the interaction of AMSCs with nanostructured Ti alloys, or on their capability to grow and differentiate into osteoblasts on these supports. Therefore, this study has the prerogative to investigate, for the first time, both the role of nanofeatures of Ti13Nb13Zr on supporting the osteogenic differentiation and activity and the effects of the two nanostructured Ti alloys (Ti6Al4V and Ti13Nb13Zr) on the growth, adhesion and osteoblast differentiation and activity of the non classical tissue-derived human AMSC.

Non-induced AMSCs are less committed to the osteoblastic lineage than non-induced NHOst control cells, and they have been shown to possess a greater proliferative potential. All the analysed PA cell lines also demonstrated the capability of maintaining a constant increase of ALP activity even 40 days after osteogenic induction, as well as a constant increase in the deposition of mineral calcium even 60 days after osteogenic induction, with respect to NHOst control cells. These data confirm the human AMSCs as an excellent source of osteoblast precursors and promising cells for bone tissue engineering applications and reconstruction of bone defects.

No statistically significant difference was shown of growth and viability of both AMSCs and NHOst cells cultured on Ti alloys compared to PS. Conversely, AMSC and NHOst adhesion is higher on both the Ti alloys than on PS. The analysis of focal adhesion contacts of AMSC and NHOst cells, at 4 days after osteogenic induction, revealed a higher degree of adhesion on both Ti alloys than on PS, confirming data by a study of Sinha et al. (27) in which primary human osteoblasts cultured on Ti6Al4V were found to adhere in greater numbers to Ti than to PS. In addition, they found that osteoblasts cultured on Ti6Al4V were significantly larger and spread better with peripherally located focal contacts due to enhanced cytoskeleton organization. Conversely, our results showed a similar cytoskeleton organization in all cell lines grown on Ti6Al4V or on PS. AMSCs and NHOst cells cultured on Ti13Nb13Zr presented an increased number of β-actin bundles, mainly localized along the lateral borders of the cells. Cells cultured on Ti13Nb13Zr also showed a higher presence of the adhesion protein vinculin. The major adhesion of both AMSCs and NHOst on Ti13Nb13Zr with respect to PS and Ti6Al4V was also confirmed by the evaluation of *FCA/TCA* ratio. These data, together with the fact that Ti13Nb13Zr does not contain vanadium, may suggest Ti13Nb13Zr as a more suitable biomaterial for human orthopaedic devices/implants, with respect to the currently used Ti6Al4V.

Both AMSCs and NHOst showed a significantly reduced ALP activity when cultured on Ti6Al4V and Ti13Nb13Zr with respect to PS. However, AMSC osteoblast activity in terms of mineral calcium deposition (evaluated both by calcein staining and Alizarin Red S assay) were comparable to that obtained on PS until 20 days from induction, and, at 40 days after osteogenic induction, also significantly higher on the two Ti alloys. The presence of good osteoblast activity of AMSCs grown on Ti6Al4V and Ti13Nb13Zr was also confirmed by an unaltered synthesis of two bone extracellular matrix proteins (COLIA1 and OCN) and an enhanced synthesis of OPN, with respect to the same cell lines cultured on PS. No difference in calcium deposition and bone matrix pro-

tein synthesis of AMSCs was observed between Ti6Al4V and Ti13Nb13Zr. Conversely, NHOst cells showed a reduced calcium deposition when cultured on both Ti6Al4V and Ti13Nb13Zr with respect to PS, while no difference has been detected in the production of bone matrix proteins in NHOst cells cultured on biomaterials or PS.

All these data confirm AMSCs as a rapidly expanding osteoblast progenitor population able to differentiate into the osteoblast lineage, to maintain a functional osteoblast phenotype, and to produce a calcified bone matrix also when integrated with the nanostructured Ti6Al4V and Ti13Nb13Zr alloys, thus representing an appropriate set of cells for human bone repair. In addition, both nanostructured Ti6Al4V and Ti13Nb13Zr surfaces have demonstrated their osteoconductive properties since they revealed to be capable of sustaining adhesion and proliferation of human osteoblast precursors, of granting their maturation into osteoblast phenotype, and of supporting the activity of mature osteoblasts in terms of mineral calcium deposition and bone extracellular matrix protein production, after osteogenic induction.

However, a recent work showed that the osteogenic properties of nanostructured Ti6Al4V are strongly associated to the different stage of osteogenic differentiation, with human primary osteoblasts able to recognize the nanostructured surface and respond to it with active osteoblast functionality even in absence of osteogenic factors within the medium, while MSCs were not induced into osteoblast differentiation only by the presence of nanostructures (26). Based on the result of this study, surely the next step should be the investigation also of osteoinductive properties of both nanostructured Ti6Al4V and Ti13Nb13Zr on AMSCs, cultured in non-osteogenic medium.

Conclusions

The present study shows that human AMSCs are able to grow, differentiate into mature osteoblasts, and produce bone tissue, when cultured on nanostructured titanium alloys in presence of osteogenic inductive factors. These cells represent an optimal source of MSCs, abundantly and easily obtainable from subcutaneous adipose tissue, for autogenous bone tissue engineering.

Importantly, the evidence of osteointegration and osteoconductive properties of nanostructured Ti6Al4V and Ti13Nb13Zr Ti alloys opens new avenues for the design of efficient Ti-based biocompatible stable scaffolds for stem cell-based bone tissue regeneration in osteoarticular, skeletal, maxillofacial, and dental disorders.

Acknowledgements

This study was supported by unrestricted grants from Fondazione Ente Cassa di Risparmio di Firenze and from Fondazione F.I.R.M.O. Raffaella Becagli to M.L. Brandi.

The Authors confirm that there are no known conflicts of interest associated with this publication and there has been no significant financial support for this study that could have influenced its outcome.

References

1. Jäger M, Zilkens C, Zanger K, et al. Significance of nano- and microtopography for cell-surface interactions in orthopaedic implants. J Biomed Biotechnol. 2007;2007(8):69036.
2. Meredith DO, Eschbach L, Riehle MO, et al. Microtopography of metal surfaces influence fibroblast growth by modifying cell shape, cytoskeleton, and adhesion. J Orthop Res. 2007;25(11):1523-1533.
3. Anselme K, Bigerelle M. Topography effects of pure titanium substrates on human osteoblast long-term adhesion. Acta Biomaterialia. 2005;1 (2):211-222.
4. Anselme K, Bigerelle M. Statistical demonstration of the relative effect of surface chemistry and roughness on human osteoblast short-term adhesion. J Mater Sci Mater Med. 2006;17(5):471-479.
5. Anselme K, Noël B, Hardouin P. Human osteoblast adhesion on titanium alloy, stainless steel, glass and plastic substrates with same surface topography. J Mater Sci Mater Med. 1999;10(12):815-819.
6. Bigerelle M, Anselme K. Statistical correlation between cell adhesion and proliferation on biocompatible metallic materials. J Mater Sci Mater Med Part A. 2005;72(1):36-46.
7. Bigerelle M, Anselme K. A kinetic approach to osteoblast adhesion on biomaterial surface. J Mater Sci Mater Med Part A. 2005;75(3):530-540.
8. Meyer U, Büchter A, Wiesmann HP, et al. Basic reactions of osteoblasts on structured material surfaces. Eur Cells Mater. 2005;9:39-49.
9. Bigerelle M, Anselme K, Dufresne E, et al. An unscaled parameter to measure the order of surfaces: a new surface elaboration to increase cells adhesion. Biomolecular Engineering. 2002;19(2-6):79-83.
10. Zreiqat H, Valenzuela SM, Nissan BB, et al. The effect of surface chemistry modification of titanium alloy on signalling pathways in human osteoblasts. Biomaterials. 2005;26(36): 7579-7586.
11. Niinomi M, Hattori T and Niwa S. Material characteristics and biocompatibility of low rigidity titanium alloys for biomedical applications. In: Jaszemski MJ, Trantolo DJ, Lewandrowski KU, Hasirci V, Altobelli DE and Wise DL (eds). Biomaterials in Orthopaedics. New York: Marcel Dekker, 2004: 41-62.
12. Olivares-Navarrete R, Hyzy SL, Hutton DL, et al. Direct and indirect effects of microstructured titanium substrates on the induction of mesenchymal stem cell differentiation towards the osteoblast lineage. Biomaterials. 2010;31(10):2728-2735.
13. Curtis ASG, Wilkinson C. Nantotechniques and approaches in biotechnology. Trends Biotechnol. 2001;19(3):97-101.
14. Curtis ASG, Wilkinson C. New depths in cell behaviour: reactions of cells to nanotopography. Bioch Soc Sympos. 1999;65:15-26.
15. Dalby MJ, Yarwood SJ, Riehle MO, et al. Increasing fibroblast response to materials using nanotopography: morphological and genetic measurements of cell response to 13-nm-high polymer demixed islands. Experimental Cell Res. 2002;276(1):1-9.
16. Scotchford CA, Ball M, Winkelmann M, et al. Chemically patterned, metal-oxide-based surfaces produced by photolithographic techniques for studying protein- and cell-interactions—II: protein adsorption and early cell interactions. Biomaterials. 2003;24(7):1147-1158.
17. Ward BC, Webster TJ. The effect of nanotopography on calcium and phosphorus deposition on metallic materials in vitro. Biomaterials. 2006;27(16):3064-3074.
18. Ward BC, Webster T. Effect of metal substrate nanometer topography on osteoblast metabolic activities. MRS proceedings 2004 Biol Bioinspired Materials Dev. 2004;823:249-254.
19. Tognarini I, Sorace S, Zonefrati R, et al. In vitro differentiation of human mesenchymal stem cells on Ti6Al4V surfaces. Biomaterials. 2008;29 (7):809-824.
20. Hunter A, Archer CW, Walker PS, et al. Attachment and proliferation of osteoblasts and fibroblasts on biomaterials for orthopaedic use. Biomaterials. 1995;16:287-295.
21. Carpenter AE, Jones TR, Lamprecht MR, et al. CellProfiler: image analysis software for identifying and quantifying cell phenotypes. Genome Biol. 2006;7:R100.
22. Arrington ED, Smith WJ, Chambers HG, et al. Complications of iliac crest bone graft harvesting. Clin Orthop. 1996;329:300-309.
23. Okazaki Y, Nishimura E. Effect of metal released from Ti alloy wear powder on cell viability. Mater Trans JIM. 2000;41:1247-1255.
24. Liu P, Smith J, Ayers DC, et al. Surface mineralization of Ti6Al4V substrates with calcium apatites for the retention and local delivery of recombinant human bone morphogenetic protein-2. Acta Biomaterialia. 2011;7:3488-3495.

25. Bigi A, Nicoli-Aldini N, Bracci B, et al. In vitro culture of mesenchymal cells onto nanocrystalline hydroxyapatite-coated Ti13Nb13Zr alloy. J Biomed Mater Res A. 2007;82(1):213-221.
26. Gittens RA, Olivares-Navarrete R, McLachlan T, et al. Differential responses of osteoblast lineage cells to nanotopographically-modified, microroughned titanium-aluminium-vanadium alloy surfaces. Biomaterials. 2012;33(35):8986-94,
27. Sinha RK, Morris F, Shah SA, et al. Surface composition of orthopaedic implant metals regulates cell attachment, spreading, and cytoskeletal organization of primary human osteoblasts in vitro. Clin Orthop Relat Res. 1994;305:258-272.